Available online at www.sciencedirect.com
ScienceDirect
Progress in Natural Science 19 (2009) 955–962
Progress in Natural Science
www.elsevier.com/locate/pnsc

Information extraction and CT reconstruction of liver images based on diffraction enhanced imaging

Chunhong Hu [a,b], Tao Zhao [a], Lu Zhang [a], Hui Li [a], Xinyan Zhao [c], Shuqian Luo [a,*]

[a] College of Biomedical Engineering, Capital Medical University, Beijing 100069, China
[b] National Laboratory of Pattern Recognition, Institute of Automation, Chinese Academy of Sciences, Beijing 100080, China
[c] Liver Research Center, Beijing Friendship Hospital, Capital Medical University, Beijing 100050, China

Received 3 April 2008; received in revised form 22 April 2008; accepted 25 June 2008

Abstract

X-ray phase-contrast imaging (PCI) is a new emerging imaging technique that generates a high spatial resolution and high contrast of biological soft tissues compared to conventional radiography. Herein a biomedical application of diffraction enhanced imaging (DEI) is presented. As one of the PCI methods, DEI derives contrast from many different kinds of sample information, such as the sample's X-ray absorption, refraction gradient and ultra-small-angle X-ray scattering (USAXS) properties, and the sample information is expressed by three parametric images. Combined with computed tomography (CT), DEI-CT can produce 3D volumetric images of the sample and can be used for investigating micro-structures of biomedical samples. Our DEI experiments for liver samples were implemented at the topography station of Beijing Synchrotron Radiation Facility (BSRF). The results show that by using our provided information extraction method and DEI-CT reconstruction approach, the obtained parametric images clearly display the inner structures of liver tissues and the morphology of blood vessels. Furthermore, the reconstructed 3D view of the liver blood vessels exhibits the micro blood vessels whose minimum diameter is on the order of about tens of microns, much better than its conventional CT reconstruction at a millimeter resolution. In conclusion, both the information extraction method and DEI-CT have the potential for use in biomedical micro-structures analysis.

Keywords: Diffraction enhanced imaging; Computed tomography; Information extraction; X-ray; Liver

1. Introduction

X-ray imaging techniques have been developed successfully in medical, biological and material research fields since Roentgen's discovery of the X-ray in 1895. Conventional radiography is based on absorption contrast mechanisms and geometrical optics, and it derives contrast from differences in X-ray absorption. However, the differences in the X-ray absorption coefficients of the structures in biological soft tissues are quite small and thus this technique may achieve low contrast and spatial resolution. X-ray phase-contrast imaging (PCI) is a new imaging technique that exploits a contrast mechanism based on differences in the X-ray refractive index distribution of a sample [1–3]. Compared with conventional radiography, PCI can increase the spatial resolution of the image about 1000 times for soft tissues, and can clearly display the inner details and structures of biological samples, which are not detectable by use of conventional radiography [2,3]. Thus, PCI has significant value and perspective in biological and medical applications.

At present, the main methods for acquiring phase information include interferometry [2–4], diffraction enhanced imaging (DEI) [5–7], and in-line holography or Fresnel diffraction [8]. Among these different PCI techniques, DEI has been widely studied and applied by scientists in many fields since Chapman et al. [5] presented the original DEI

* Corresponding author. Tel.: +86 10 83911566; fax: +86 10 84719024.
E-mail address: sqluo@ieee.org (S. Luo).

1002-0071/$ - see front matter © 2009 National Natural Science Foundation of China and Chinese Academy of Sciences. Published by Elsevier Limited and Science in China Press. All rights reserved.
doi:10.1016/j.pnsc.2008.06.031

method and gave the calculation equations of the apparent absorption image and refraction image. DEI can generate contrast from a sample's X-ray absorption, refraction and ultra-small-angle X-ray scattering (USAXS) properties, and it utilizes an analyzer crystal with high angular sensitivity to measure the three contrasts of the sample, which dramatically improves the contrast and spatial resolution of the images. Utilizing the information extraction method, three parametric images can be obtained that depict, respectively, the effects of absorption, refraction and USAXS produced by the sample [9–15]. The parametric images can be used to better display the inner structures and details of the sample, and they can also be fused or combined together to obtain several kinds of information in one image according to the characteristics of the parametric images and the specificities of the sample. In recent years, the information extraction in DEI attains widespread studies and applications in biological and medical fields, such as breast cancer diagnosis, and cartilage imaging [9,16,17]. Although the parametric images provide a rich description of the sample's details, they are two-dimensional (2D) images that represent projections of the three-dimensional (3D) distributions of the sample's physical properties. Diffraction enhanced imaging computed tomography (DEI-CT) can produce 3D volumetric images of the sample, and can reveal 3D structures of the sample. DEI-CT exhibits excellent results with many significant additional advantages over conventional absorption-based CT, and displays internal structures of organs or soft tissues on the order of microns [18–21].

The liver imaging study is an important part in medical imaging, and it can assist in liver disease diagnosis. Although conventional radiography, CT and magnetic resonance imaging (MRI) can be used to observe some serious pathological changes, the micro-structures of liver tissues are invisible to these techniques due to the restrictions of their spatial resolution and contrast. To date, liver disease diagnosis has mainly relied on liver biopsy, which has remained the gold standard for the evaluation of the severity of liver disease. However, liver biopsy is invasive and associated with a relatively high risk of complications. The DEI and DEI-CT can clearly display micro-structures of the sample with the advantages of high contrast and spatial resolution, thus they can compensate for the deficiencies of the above-mentioned techniques. In this work, the DEI technique is applied to rat liver imaging, and the parametric images and 3D structures of the liver sample are obtained using the information extraction method and DEI-CT, respectively.

2. Principle of DEI

The DEI setup is sketched in Fig. 1, and it is composed of two perfect crystals' monochromator-analyzer system with a sample placed between them [7]. The monochromator crystal is used to select the energy range of the X-ray from the incident synchrotron beam and to generate a nearly monochromatic X-ray beam [5]. The monochromatic X-ray beam transmitted through the sample is incident upon the analyzer crystal, and the intensity of the X-ray beam reflected by the analyzer crystal is measured by a detector, which results in the formation of a DEI image [5]. In the meridian plane, the analyzer crystal can be rotated within an angle range of the order of micro-radians away from the monochromator crystal. The rocking curve (RC) of the DEI system describes the reflectivity of the analyzer crystal as a function of the incident angle, as shown in Fig. 2, in which the triangle labels indicate the selected points on the RC in DEI imaging. According to Bragg's diffraction law, only the X-ray satisfying the Bragg condition of the analyzer crystal will be reflected onto the detector. In the energy range of the hard X-ray, the full width half maximum (FWHM) of the analyzer RC is about a few micro-radians, which is approximately equal to the Darwin width of the crystal, so the analyzer crystal has a high angular sensitivity. The basis of DEI depends on the absorption, refraction and scattering properties of the sample and is determined by the analyzer crystal. The diffracted intensity is picked up by setting the angle of the analyzer crystal. The observed DEI intensity can be given by

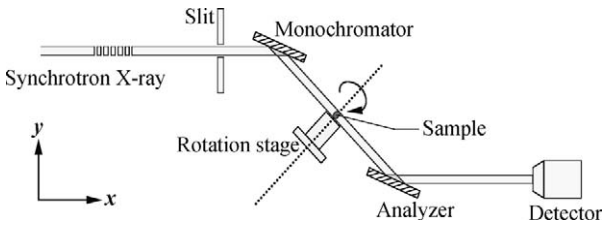

Fig. 1. The DEI setup.

$$I = I_R R(\theta_A + \Delta\theta) \tag{1}$$

where $R(\theta)$ is the analyzer reflectivity; θ_A is the setting angle of the analyzer crystal; I_R is the apparent absorption intensity; and $\Delta\theta$ is the refraction angle of the X-ray passed through the sample in the meridian plane [5].

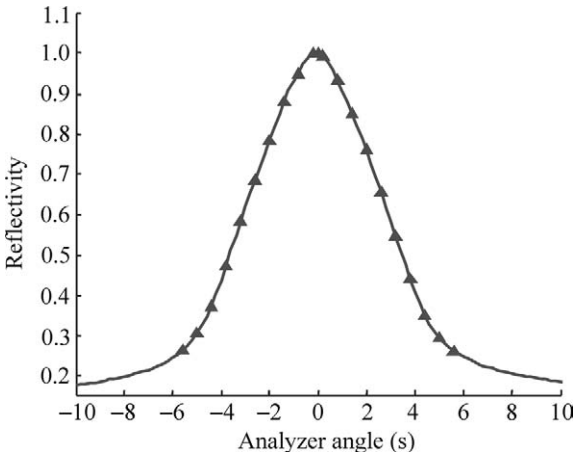

Fig. 2. The RC in the experiment.

3. The DEI information extraction method

When the X-ray beam transmits through a biological sample, the interactions between the X-ray and the sample are complicated, involving absorption, refraction, USAXS, and so on. In conventional radiography, the undesired scattering degrades the image, and the X-ray refraction inside the sample is also not detectable. The DEI technique utilizes the analyzer crystal with an acceptance angle range of only a few micro-radians. The high angular sensitivity of the crystal allows the X-ray absorption, refraction, and USAXS of the sample to be measured. DEI provides a way of imaging these contrast mechanisms. The aim of the DEI information extraction is to focus on these contrast mechanisms and consider them individually. These contrast mechanisms are used to present true absorption, refraction, USAXS images, namely the parametric images. The parametric images possess higher contrast, and they can provide more detailed information of the sample.

There has been an increasing interest in DEI information extraction methods. In 1997, using two images taken on either side of the RC of the analyzing crystal, Chapman et al. [5] presented the original information extraction method and produced images known as the apparent absorption image and refraction image. In this method, $R(\theta_A + \Delta\theta)$ can be approximated by a Taylor series expansion as follows:

$$R(\theta_A + \Delta\theta) = R(\theta_A) + \frac{\mathrm{d}R}{\mathrm{d}\theta}(\theta_A)\Delta\theta \tag{2}$$

The intensities of the images taken on the low-angle side (θ_L) and the high-angle side (θ_H) of the RC are

$$I_\mathrm{L} = I_R(R(\theta_\mathrm{L}) + \frac{\mathrm{d}R}{\mathrm{d}\theta}(\theta_\mathrm{L})\Delta\theta) \tag{3}$$

$$I_\mathrm{H} = I_R(R(\theta_\mathrm{H}) + \frac{\mathrm{d}R}{\mathrm{d}\theta}(\theta_\mathrm{H})\Delta\theta) \tag{4}$$

From Eqs. (3) and (4) given above, the apparent absorption image (I_R) and refraction image ($\Delta\theta$) can be calculated by

$$I_R = \frac{I_\mathrm{L}\left(\frac{\mathrm{d}R}{\mathrm{d}\theta}\right)(\theta_\mathrm{H}) - I_\mathrm{H}\left(\frac{\mathrm{d}R}{\mathrm{d}\theta}\right)(\theta_\mathrm{L})}{R(\theta_\mathrm{L})\left(\frac{\mathrm{d}R}{\mathrm{d}\theta}\right)(\theta_\mathrm{H}) - R(\theta_\mathrm{H})\left(\frac{\mathrm{d}R}{\mathrm{d}\theta}\right)(\theta_\mathrm{L})} \tag{5}$$

$$\Delta\theta = \frac{I_\mathrm{H}R(\theta_\mathrm{L}) - I_\mathrm{L}R(\theta_\mathrm{H})}{I_\mathrm{L}\left(\frac{\mathrm{d}R}{\mathrm{d}\theta}\right)(\theta_\mathrm{H}) - I_\mathrm{H}\left(\frac{\mathrm{d}R}{\mathrm{d}\theta}\right)(\theta_\mathrm{L})} \tag{6}$$

The method is applied on a pixel-by-pixel basis, and it is very simple to calculate. Moreover, the method decreases imaging time and the X-ray radiation dose of the sample due to the need for just two DEI images, which is very important in biomedical imaging applications. However, the method has some drawbacks: (1) it does not account for USAXS and therefore the apparent absorption image and refraction image will generally contain artifacts when imaging samples produce such scattering; (2) the Taylor approximation of the RC limits its applicability and decreases the obtained refraction angle range; (3) the analyzer needs to be set to the 50% reflectivity points on either side of the RC so as to obtain two DEI images at low and high angle sides, which it actually has difficulty in doing.

Multiple image radiography (MIR) is a significant improvement over DEI based on a statistical analysis, and it can produce true absorption, refraction and USAXS images, respectively [9–11]. Compared with the information extraction method proposed by Chapman et al. [5], the main advantages of MIR are as follows: (1) MIR produces an additional USAXS image; (2) MIR corrects substantial errors inherent in DEI and produces more accurate refraction and absorption images; and (3) MIR is more robust to noise [9]. However, MIR increases the imaging time and X-ray radiation dose of the sample due to the need for more DEI images.

In MIR, two series of DEI images are acquired in N ($N \geqslant 3$) positions of the RC, one with the sample and one without the sample, and they give, respectively, for each individual pixel, a sample RC and a background RC. Here, $I_\mathrm{s}(\theta_n)$ ($n = 1, 2, \ldots, N$) denotes the intensity of the DEI image in the position θ_n of the RC with the sample. $I_\mathrm{b}(\theta_n)$ denotes the intensity of the DEI image in the position θ_n of the RC without the sample. The MIR absorption image is similar to a conventional radiograph, but exhibits much greater contrast owing to the scattering rejection. The absorption information of the sample can be given by

$$I_\mathrm{abs} = -\ln\frac{\sum_{n=1}^{N} I_\mathrm{s}(\theta_n)}{\sum_{n=1}^{N} I_\mathrm{b}(\theta_n)} \tag{7}$$

Refraction induces an overall deflection of the beam that produces an angular shift of the beam centroid when compared to its position in the absence of the sample [9,18]. Because the angular shift of the beam centroid is only due to the refraction phenomena, the MIR refraction image of the sample can be expressed as follows:

$$\Delta\theta = \theta_\mathrm{s} - \theta_\mathrm{b} = \frac{\sum_{n=1}^{N} I_\mathrm{s}(\theta_n)\theta_n}{\sum_{n=1}^{N} I_\mathrm{s}(\theta_n)} - \frac{\sum_{n=1}^{N} I_\mathrm{b}(\theta_n)\theta_n}{\sum_{n=1}^{N} I_\mathrm{b}(\theta_n)} \tag{8}$$

The MIR USAXS image quantifies angular divergence of the beam caused by the presence of textural structures in the sub-pixel length scale, and it can be given by

$$\sigma_\theta^2 = \frac{1}{\sum_{n=1}^{N} I_\mathrm{s}(\theta_n)} \sum_{n=1}^{N} [\theta_n - \theta_\mathrm{s}]^2 I_\mathrm{s}(\theta_n) - \frac{1}{\sum_{n=1}^{N} I_\mathrm{b}(\theta_n)} \times \sum_{n=1}^{N} [\theta_n - \theta_\mathrm{b}]^2 I_\mathrm{b}(\theta_n) \tag{9}$$

4. Principle of DEI-CT

The parametric images and DEI images are still the 2D images, thus the structures of the sample are overlapped in these images and cannot display the structure details of the sample. To solve this problem, 3D volumetric images of the sample can be produced by use of CT, and it can display

3D inner structures of the sample. Therefore, the high-resolution CT technique has now become an important tool for biological research.

In conventional radiography, the observed intensity in the detector can be given by

$$I = I_0 \exp\left[-\int_0^t \mu(x,y,z)\mathrm{d}z\right] \tag{10}$$

where I_0 is the X-ray incident intensity, and μ is the absorption coefficient; (x, y, z) represents the coordinate system, and t is the thickness of the sample. In DEI, when the analyzer is set at the peak position of the RC, the observed intensity on the detector, namely the peak image can approximately be represented as

$$I = I_0 \exp\left[-\int_0^t \mu(x,y,z)\mathrm{d}z - \int_0^t \chi(x,y,z)\mathrm{d}z\right] \tag{11}$$

where χ is the extinction coefficient [19,20]. Eqs. (10) and (11) have consistent mathematical expressions, and the peak image can be expressed as line integrals of the absorption and extinction coefficient. Thus, based on the peak image, conventional CT reconstruction approaches, such as the filter back projection (FBP) approach, can be used to reconstruct CT images. Note that the DEI-CT in this paper especially denotes the CT based on the peak image in DEI. Actually, due to the presence of the extinction contrast caused by the scattering rejection, the peak image in DEI has higher contrast than that in the conventional radiograph, which in turn makes DEI-CT possess higher contrast than the conventional absorption-based CT. Therefore, the 3D micro-structures of the sample can be obtained by use of DEI-CT.

5. Experimental results

5.1. The setups and samples

The experiments were performed at the 4W1A beamline of Beijing Synchrotron Radiation Facility (BSRF). As shown in Fig. 1, the double-crystal DEI setup was used in the experiments. Two perfect Si(111) crystals were used as the monochromator and analyzer. The tunable energy range of the X-ray beam was 3–22 keV, and the X-ray beam energy was set at 12 keV. The detector had an X-ray FDI-18 mm camera system (Photonic Science Ltd.) with 1300×1030 pixels, and $10.9 \times 10.9\ \mu m^2$ per pixel, with a field of view of $20 \times 10\ mm^2$. The rat liver tissue was selected as the sample and was preserved in formalin prior to imaging. Two series of DEI images were acquired in 21 positions of the RC, one with the sample and one without the sample, and they could be used to obtain absorption, refraction, and USAXS images. In CT imaging, a total of 180 projection images of the sample were obtained in a 1.0° step within 180° when the analyzer was set at the peak position of the RC, and the sample was placed in a plastic container in order to avoid the deformation of the sample due to too much exposure.

Fig. 3. The conventional radiograph of the liver.

5.2. Conventional radiography

In the DEI setup, the conventional radiography experimental setup based on the synchrotron source was constructed by setting the monochromator and analyzer crystals parallel, and placing the sample behind two crystals and close to the detector. The conventional radiograph of the liver is shown in Fig. 3. Because the differences in linear attenuation coefficients between soft tissues are usually small and the undesired scattering blurs the image, the contrast of Fig. 3 is very low and the structures of the liver sample cannot be displayed clearly.

5.3. The apparent absorption image and refraction image

Combining numerically two images recorded with the analyzer set to the 50% reflectivity points on either side of the RC, the apparent absorption image and refraction image can be calculated using Eqs. (5) and (6). Fig. 4(a)

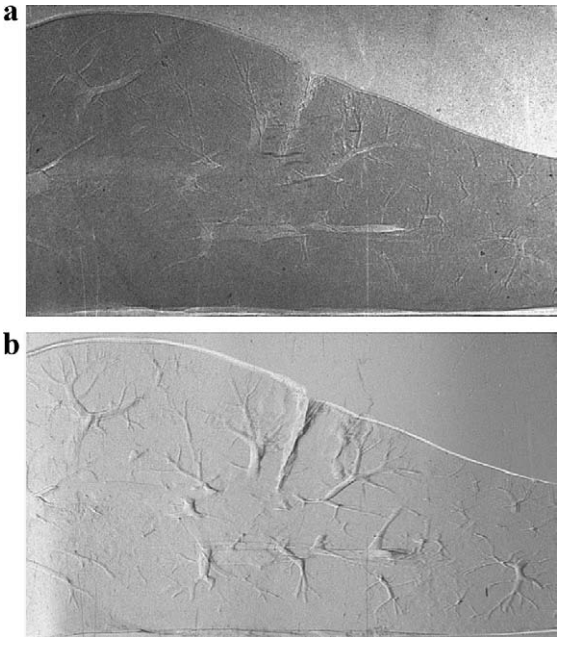

Fig. 4. The images of the liver. (a) The apparent absorption image; (b) the refraction image.

and (b) show the apparent absorption image and refraction image of the liver sample, respectively. The apparent absorption image is similar to a conventional radiograph, but exhibits much greater contrast owing to the scattering rejection. However, the apparent absorption image cannot still display the structures of the liver sample due to small differences in linear attenuation coefficients between soft tissues. As shown in Fig. 4(b), the refraction image has a much superior contrast compared with the images in Figs. 3 and 4(a), and shows a marked edge enhancement effect, which results in an obvious 3D visual effect. In Fig. 4(b), the blood vessel and its peripheral branches can be clearly displayed, and the minimum blood vessel diameter is on the order of microns, which is almost impossible without the use of contrast agents in conventional radiography. Therefore, the refraction image can be effectively utilized to assist in liver disease diagnosis due to the advantages of high contrast, high spatial resolution and the distinct edge enhancement effect.

5.4. The parametric images in MIR

Fig. 5(a), (b) and (c) show absorption, refraction and USAXS images of the liver sample, respectively. All three images have good contrast, especially for refraction and USAXS images. Similar to Fig. 4(b), the refraction image shown in Fig. 5(b) can also reveal the trees of blood vessels with the minimum blood vessel diameter of the order of microns, which provides possibilities for investigation of the vascular system. Moreover, a better signal to noise ratio (SNR) can be obtained in Fig. 5(b), and the SNR in Fig. 4(b) is quite poor because of the influence of stochastic noise. The SNR values in Figs. 4(b) and 5(b) are equal to 17.4 and 62.5, respectively. The USAXS image is a new image produced by MIR, and it conveys the presence of micro-structures in the sample, thus differentiating homogeneous tissues from tissues that are irregular on a scale of microns. As expected, the USAXS image shown in Fig. 5(c) can clearly display the blood vessel structures. The DEI method, namely the information extraction method proposed by Chapman et al. [5] does not consider the USAXS, thus it will produce erroneous results when USAXS is present, which is actually always the case in biological tissues [9].

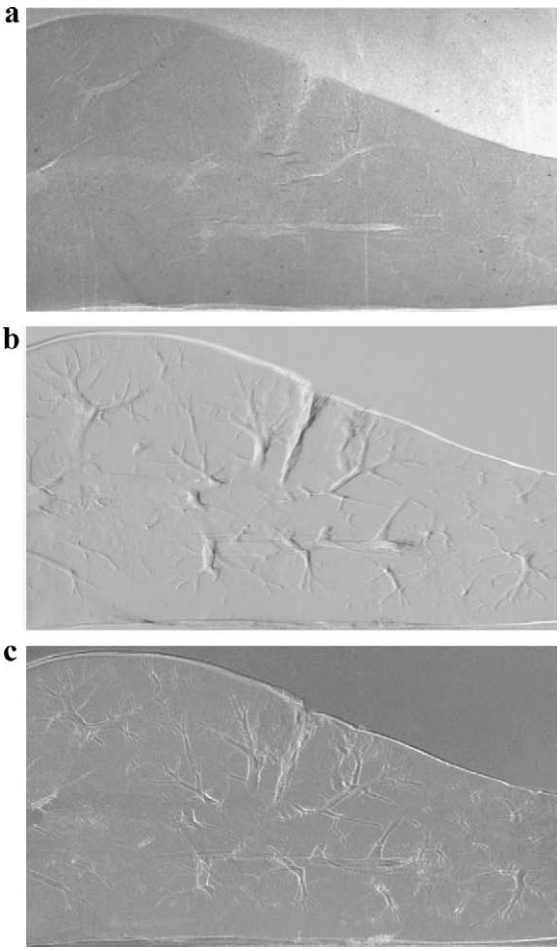

Fig. 5. The MIR parametric images of the liver. (a) The absorption image; (b) the refraction image; (c) the USAXS image.

5.5. The 3D reconstruction of blood vessels

Conventionally, the 3D reconstruction of blood vessels in the liver sample relies on histological methods such as histological sections. The histological sections provide a way to directly observe the inner details of the biological

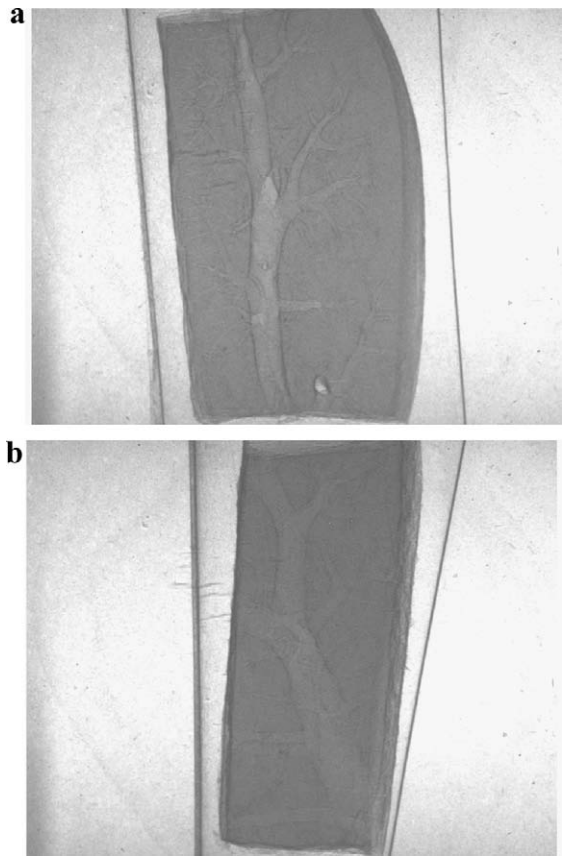

Fig. 6. Two projection images of the liver at different angles.

tissues with a high spatial resolution. However, they have some inherent limitations. First, the histological sections destroy the integrity of the liver. Second, the procedures of the histological sections are rather complicated and time-consuming due to the need for image registration and segmentation. The DEI-CT can circumvent these limitations of histological methods. Moreover, the DEI-CT can clearly reveal inner micro-structure details of the liver with a high contrast and spatial resolution.

A CT image can be reconstructed to display the inner structures of the sample using projection images at different angles. Fig. 6(a) and (b) show two projection images of the liver sample at different angles, and Fig. 7(a) and (b) are corresponding CT images. For the estimation of the blood vessel diameter in the CT image of the liver sample, a polystyrene phantom can be used to reconstruct the CT image under the same condition. There are two air-filled cylindrical channels and one air-filled solid square channel in the phantom, and the diameters and side of the channels on the cross section perpendicular to their axis are 496 μm, 323 μm and 511 μm, respectively. Fig. 7(c) is the CT image of the phantom. Fig. 7(d) is obtained by combining the CT image of the liver sample and CT image of the phantom. In Fig. 7(d), the minimum blood vessel diameter is about one tenth of the phantom's circular hole, and the diameter of the phantom's hole is about 500 μm. Thus, the minimum blood vessel diameter is about 50–60 μm.

In order to avoid massive data processing and save computation time, a rectangular area of interest has been selected from the reconstructed CT image, and it is stored as the image of 592 × 466 pixels. The approach of DEI-CT is described as below:

1. Preprocess the projection images of DEI. The noise filter is utilized to suppress noise, and the background image is used for normalization.
2. Obtain the CT image and extract the profile of the liver area by the use of image segmentation.
3. Enhance the image and highlight the edge of the blood vessels.
4. Reconstruct 3D structures of blood vessels by use of the Amira software.

The 3D renderings of blood vessels are shown in Fig. 8. The 3D image clearly depicts the structure of vessel branching, vessel trend and vessel morphology in the trees of

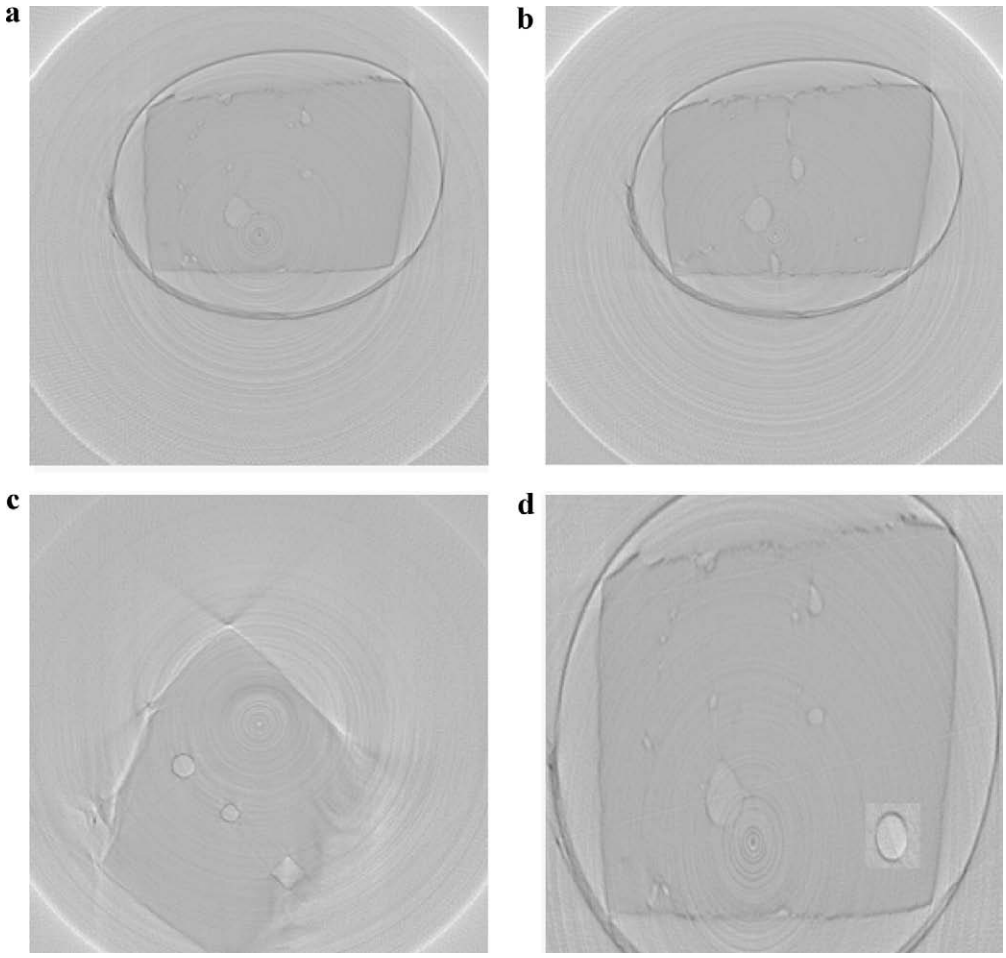

Fig. 7. The CT images. (a) and (b) show two CT images of the liver; (c) the CT image of the phantom; (d) the CT image of the phantom and liver combined together.

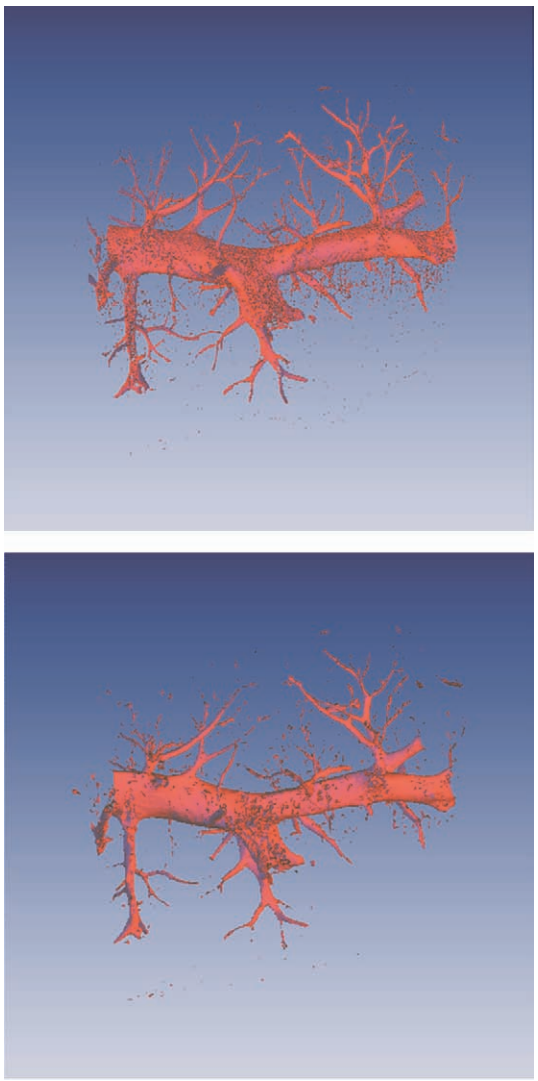

Fig. 8. Two profiles of the 3D reconstruction of blood vessels.

blood vessels, and the minimum blood vessel diameter is about 50 μm. After 3D reconstruction, the inner micro-structures of the blood vessels can be observed on a computer by the use of different view angles, which provides a good way to observe the blood vessels of the liver.

6. Discussion and conclusion

The spatial resolution of advanced CT and MRI reaches about 0.5 mm, and the spatial resolution of positron emission tomography (PET) is about 5 mm. However, they are not high enough for clinical applications in disease diagnosis. Thus, the micro-structures of the sample are invisible to these techniques. Conventional liver observation depends on histological examinations. However, histological diagnoses have some inherent limitations such as their destructiveness and complexity. Compared with it, the DEI and DEI-CT techniques are simple and non-destructive. Moreover, due to the advantages of high contrast and spatial resolution, the DEI and DEI-CT techniques will be effective and useful in liver disease diagnosis.

In this work, we use the information extraction method based on DEI images to obtain parametric images that depict the effects of absorption, refraction and USAXS produced by the liver sample. Compared with the conventional radiograph, the parametric images have a higher contrast. Especially, the refraction image shows a marked edge enhancement effect, and reveals the trees of blood vessels with the minimum blood vessel of several microns. However, the parametric images and DEI images are still the 2D images. In order to circumvent the limitation, the DEI-CT technique has been used to reconstruct the 3D structures of blood vessels. The 3D image clearly shows the micro-structures of blood vessels, and the minimum blood vessel diameter is about 50 μm.

In this study, the isolated rat liver sample was used as subject of the experiments. In the future, research of human liver or other biological tissues *in vivo* will be conducted. Therefore, the information extraction method based on DEI images and DEI-CT will have extensive application prospects in medical diagnoses.

Acknowledgements

This work was supported by the National Natural Science Foundation of China (Grant Nos. 60532090 and 30770593) and the National Laboratory of Pattern Recognition, Institute of Automation, Chinese Academy of Sciences, China (Grant No. 07-21-9). The authors thank Prof. Zhu Peiping, Dr. Yuan Qingxi, Dr. Huang Wanxia and Dr. Wang Junyue from BSRF for their assistance in our experiments.

References

[1] Davis TJ, Gao D, Gureyev TE, et al. Phase-contrast imaging of weakly absorbing materials using hard X-rays. Nature 1995;373(6515):595–8.
[2] Momose A, Fukuda J. Phase-contrast radiographs of non-stained rat cerebellar specimen. Med Phys 1995;22(4):375–9.
[3] Momose A, Takeda T, Itai Y, et al. Phase-contrast X-ray computed tomography for observing biological soft tissues. Nat Med 1996;2(4):473–5.
[4] Momose A. Phase-sensitive imaging and phase tomography using X-ray interferometers. Opt Express 2003;11(19):2303–14.
[5] Chapman D, Thomlinson W, Johnston RE, et al. Diffraction enhanced X-ray imaging. Phys Med Biol 1997;42(11):2015–25.
[6] Dilmanian FA, Zhong Z, Ren B, et al. Computed tomography of X-ray index of refraction using the diffraction enhanced imaging method. Phys Med Biol 2000;45(4):933–46.
[7] Li G, Wang N, Wu ZY. Hard X-ray diffraction enhanced imaging only using two crystals. Chin Sci Bull 2004;49(20):2120–5.
[8] Wilkins SW, Gureyev TE, Gao D, et al. Phase-contrast imaging using polychromatic hard X-rays. Nature 1996;384(6607):335–8.
[9] Wernick MN, Wirjadi O, Chapman D, et al. Multiple-image radiography. Phys Med Biol 2003;48(23):3875–95.
[10] Pagot E, Cloetens P, Fiedler S, et al. A method to extract quantitative information in analyzer-based X-ray phase contrast imaging. Appl Phys Lett 2003;82(20):3421–3.

[11] Oltulu O, Zhong Z, Hasnah M, et al. Extraction of extinction, refraction and absorption properties in diffraction enhanced imaging. J Phys D Appl Phys 2003;36(17):2152–6.
[12] Chou CY, Anastasio MA, Brankov JG, et al. An extended diffraction-enhanced imaging method for implementing multiple-image radiography. Phys Med Biol 2007;52(7):1923–45.
[13] Rigon L, Besch H, Arfelli F, et al. A new DEI algorithm capable of investigating sub-pixel structures. J Phys D Appl Phys 2003;36(10A):A107–12.
[14] Rigon L, Arfelli F, Menk RH. Three-image diffraction enhanced imaging algorithm to extract absorption, refraction, and ultrasmall-angle scattering. Appl Phys Lett 2007;82(20):3421–3.
[15] Rigon L, Arfelli F, Menk RH. Generalized diffraction enhanced imaging to retrieve absorption, refraction and scattering effects. J Phys D Appl Phys 2007;36(17):3077–89.
[16] Muehleman C, Li J, Zhong Z, et al. Multiple-image radiography for human soft tissue. J Anat 2006;208(1):115–24.
[17] Liu CL, Yan XH, Zhang XY, et al. Evaluation of X-ray diffraction enhanced imaging in the diagnosis of breast cancer. Phys Med Biol 2007;52(2):419–27.
[18] Brankov JG, Wernick MN, Yang YY, et al. Computed tomography implementation of multiple-image radiography. Med Phys 2006;33(2):278–89.
[19] Shu H, Zhu PP, Wang JY, et al. Diffraction enhanced imaging computer tomography. Acta Phys Sin 2006;55(3):1099–106, [in Chinese].
[20] Yuan QX, Wang JY, Zhu PP, et al. Computerized tomography using peak-position image of diffraction enhanced imaging. High Energ Phys Nuc 2005;29(10):1023–6, [in Chinese].
[21] Yin HX, Zhao T, Liu B, et al. Visualization of guinea pig cochleae with computed tomography of diffraction enhanced imaging and comparison with histology. J X-ray Sci Technol 2007;15(2):73–84.